

High Surface Area Conjugated Microporous Polymers: The Importance of Reaction Solvent Choice

Robert Dawson, Andrea Laybourn, Yaroslav Z. Khimyak, Dave J. Adams, and Andrew I. Cooper*

Department of Chemistry and Centre for Materials Discovery, University of Liverpool, Crown Street, Liverpool L69 7ZD, United Kingdom

Received July 11, 2010; Revised Manuscript Received September 12, 2010

ABSTRACT: The choice of reaction solvent has a major influence on the surface area and pore volume in conjugated microporous polymer (CMP) networks synthesized by Sonogashira–Hagihara palladium-catalyzed cross-coupling chemistry of aromatic dibromo monomers with 1,3,5-triethynylbenzene. Four solvents were evaluated for these reactions: *N,N*-dimethylformamide (DMF), 1,4-dioxane, tetrahydrofuran (THF), and toluene. Networks synthesized in DMF tend to exhibit the highest surface areas (up to 1260 m²/g), whereas those synthesized in toluene have on average significantly lower surface areas and pore volumes. By judicious choice of reaction solvent, microporous materials can be prepared which combine high surface area with a variety of functional groups of interest in applications such as gas storage, molecular separations, and catalysis.

Introduction

Microporous organic polymers are of growing interest due to their possible uses in gas adsorption,^{1–4} separations,⁵ and catalysis.^{5–7} There are several classes of microporous organic polymers. Polymers of intrinsic microporosity (PIMs)^{8–11} employ rigid, contorted monomers in order to prevent the polymer chains packing efficiently, thus creating pore volume. Linear PIMs have the unique advantage that they are solution processable. Hypercross-linked polymers (HCPs)^{3,12–16} have been prepared with BET surface areas of up to 2000 m²/g^{3,15} but require stoichiometric amounts of iron(III) chloride or other reagents for their synthesis, and this somewhat limits the potential synthetic diversity of this method. Covalent organic framework (COFs)^{17–20} are crystalline organic networks, and materials with Brunauer–Emmett–Teller (BET) surface areas of more than 4000 m²/g have been reported.¹⁸

Recently, there has been significant interest in a new class of materials dubbed as “conjugated microporous polymers” (CMPs).^{21,22} CMPs are typically prepared by metal-catalyzed cross-coupling (or homocoupling) chemistry. The distinguishing feature of CMP materials is that they combine microporosity and high surface areas with extended conjugation, suggesting a range of new applications. A broad range of CMPs have been prepared already since the first report of such materials in 2007^{21–34} including a network with a BET surface area of 5640 m²/g,³⁵ one of the highest reported for any class of material. These discoveries are now leading to exciting applications in areas such as heterogeneous catalysis,³⁶ selective guest sorption,³⁷ light-harvesting networks,³⁸ metal nanoparticle composites,³⁹ and metal-doped materials with remarkable H₂ sorption properties.^{24,40} It is therefore of significant interest to develop improved synthetic methods for preparing this class of materials.

We recently reported the introduction of a wide range of chemical functionality into the structures of CMPs using Sonogashira–Hagihara coupling.²⁸ Incorporation of different functional groups

was shown to vary surface properties, with hydrophobic or hydrophilic networks being formed depending on the monomer choice. However, not all of the monomers used in this study resulted in highly porous materials.²⁸ Additionally, the networks gave rise to either type I or type IV N₂ gas sorption isotherms according to IUPAC classifications,⁴¹ the latter indicating the presence of both micropores and mesopores or small macropores. We ascribed these results to a number of factors. First, dibromo monomers were used rather than the diiodo monomers in our previous reports.^{21,25,27,31} Brominated monomers are known to be less reactive in Sonogashira–Hagihara cross-coupling reactions,^{42,43} and it is likely that this lower reactivity influences the degree of condensation in the networks. This in turn influences the phase behavior and hence the degree of interparticulate meso- and macroporosity that is observed. Additionally, we hypothesized that the degree of solvation imparted by the porogenic solvent medium could vary with the monomer type, thus leading to variable results, although we did not test this idea. Here, we demonstrate a strong solvent effect for porosity in CMP networks prepared from a range of dibromo monomers. Such solvent porogen effects are known to direct the morphology in macroporous resins.⁴⁴ This is the first systematic study of solvent effects in CMP syntheses. Some materials show a 2-fold or even 4-fold enhancement in surface area depending on the choice of reaction solvent, suggesting that solvent should be prioritized as a study variable in the synthesis of new CMP materials.

Experimental Section

Materials. 1,3,5-Triethynylbenzene was obtained from ABCR and used as received. All other chemicals and solvents were obtained from Sigma-Aldrich and used as received. Anhydrous grade solvents were used throughout (Sigma-Aldrich). All chemicals used had a purity of 97% or greater.

Synthesis of PAE Networks. All of the networks were synthesized by palladium-catalyzed Sonogashira–Hagihara cross-coupling condensation reaction of arylethynyls and aryl halides.^{21,22,25} In a typical procedure, 1,3,5-triethynylbenzene

*Corresponding author. E-mail: aicooper@liverpool.ac.uk.

(1 mmol) and dibromomonomer (1 mmol) were placed in a Radley's 6-place carousel 100 mL round-bottom flask which was degassed and backfilled with nitrogen gas. A 1.5 M excess of ethynyl groups was used as previously described.²⁵ The solids were dissolved in a mixture of the anhydrous solvent (1.5 mL) and anhydrous triethylamine (1.5 mL) and heated to the reaction temperature. When the solution had reached this temperature, a slurry of tetrakis(triphenylphosphine)palladium(0) (50 mg, 0.04 mmol) and copper(I) iodide (15 mg, 0.08 mmol) in anhydrous solvent (1 mL) was added, and the reaction was stirred under nitrogen for 3 days. The solid product was collected by filtration and washed well with hot reaction solvent followed by methanol before being Soxhlet extracted with methanol for 16 h. The products were dried in vacuo at 60 °C for 16 h to give insoluble light to dark brown solids. Example data for network **1**. Yields: 112% (toluene), 118% (DMF), 77% (THF), and 82% (dioxane). Elemental analysis: C 78.72, H 3.45, (toluene); C 80.10, H 3.55, (DMF); C 78.81, H 3.35, N 2.42 (THF); C 75.77, H 3.42 (dioxane). FTIR: 3303 (–C≡C–H), 3056 (–C_{Ar}–H) 2208 (–C≡C–), 1582 (–C_{Ar}=C_{Ar}–).

Gas Sorption Analysis. Polymer surface areas and pore size distributions were measured by nitrogen adsorption and desorption at 77.3 K using either a Micromeritics ASAP 2420 or ASAP 2020 volumetric adsorption analyzer. The surface areas were calculated in the relative pressure (P/P_0) range from 0.01 to 0.05.²⁸ Pore size distributions and pore volumes were derived from the adsorption branches of the isotherms using the nonlocal density functional theory (NL-DFT) pore model for pillared clay with cylindrical pore geometry. Samples were degassed at 120 °C for 15 h under vacuum (10^{-5} bar) before analysis. Hydrogen isotherms were measured at 77.3 and 87.3 K up to 1.13 bar using a Micromeritics ASAP 2420 volumetric adsorption analyzer.

Infrared Spectroscopy. IR spectra were collected as KBr disks using a Bruker Tensor 27.

Solid-State NMR. Solid-state NMR spectra were measured on a Bruker Avance 400 DSX spectrometer operating at 100.61 MHz for ¹³C and 400.13 MHz for ¹H. 1D ¹H–¹³C cross-polarization magic angle spinning (CP/MAS) NMR experiments were carried out at an MAS rate of 10.0 kHz using zirconia rotors 4 mm in diameter. The ¹H $\pi/2$ pulse was 3.4 μ s, and two-pulse phase modulation (TPPM) decoupling⁴⁵ was used during the acquisition. The Hartmann–Hahn condition was set using hexamethylbenzene. The spectra were measured using a contact time of 2.0 ms and a relaxation delay of 10.0 s. Typically, 984 scans were accumulated. The values of the chemical shifts are referred to that of TMS. The analysis of the spectra (deconvolution and integration) was carried out using Bruker TOPSPIN software. ¹H–¹³C cross-polarization magic angle spinning (CP/MAS) NMR kinetics experiments were also carried out at an MAS rate of 10 kHz, and the contact time was varied from 0.01 to 16 ms. Eighteen slices were collected. A relaxation delay of 10 s was used, and 416 scans were accumulated per slice. The CP kinetics curves were fitted with either the classical ISmodel.⁴⁶

Scanning Electron Microscopy. High-resolution imaging of the polymer morphology was achieved using a Hitachi S-4800 cold field emission scanning electron microscope (FE-SEM). The dry samples were prepared on 15 mm Hitachi M4 aluminum stubs using either silver dag or an adhesive high-purity carbon tab. The samples were then coated with a 2 nm layer of gold using an Emitech K550X automated sputter coater. The FE-SEM measurement scale bar was calibrated using certified SIRA calibration standards. Imaging was conducted at a working distance of 8 mm and a working voltage of 3 kV using a mix of upper and lower secondary electron detectors.

Results and Discussion

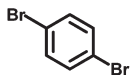
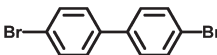
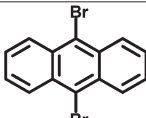
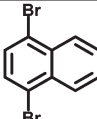
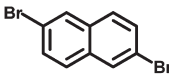
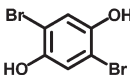
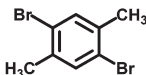
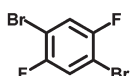
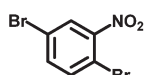
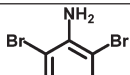
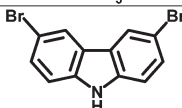
We showed previously that a wide range of monomers can be incorporated into CMP networks via the direct ($A_3 + B_2$)

palladium-catalyzed cross-coupling polycondensation of 1,3,5-triethynylbenzene and a broad range B_2 monomers.²⁸ For these reactions, we utilized a 1.5 M excess of ethynyl functionality as this was shown to lead to higher porosity in the final materials as compared to other ratios.²⁵ These polymerizations were all carried out in toluene. The alternative solvents chosen for this new study were *N,N*-dimethylformamide (DMF) and tetrahydrofuran (THF), both common solvents for Sonogashira–Hagihara reactions, as well as 1,4-dioxane which has been used for example in the synthesis of the highly porous COF networks.^{17–20,47} Reactions in THF were carried out under reflux, while those in DMF and dioxane were performed at 100 °C. Comparative reactions in toluene were also carried out at 100 °C. As described previously,²⁸ the catalyst was added to the reaction mixture after the solvent/monomer mixture had reached the required reaction temperature. In this study, we have examined a subset of the B_2 monomers described previously,²⁸ chosen in particular to cover those which previously formed networks with low BET surface areas (i.e., 9,10-dibromoanthracene, 4,4'-dibromobiphenyl, and 2,5-dibromonitrobenzene) as well as networks which contain potentially useful chemical functionality (e.g., 1,4-dibromo-2,5-difluorobenzene, 1,4-dibromo-2,5-dihydroxybenzene, 2,6-dibromo-4-methylaniline, and 3,6-dibromocarbazole). In addition, we also examined two isomers of dibromonaphthalene which were not studied previously to give a total of 11 B_2 monomers (see Table 1). In all cases, networks were produced as brown powders which were insoluble in all common solvents. The materials were recovered by filtration and washed with hot solvent (i.e., the same solvent as used in the reaction), followed by exhaustive Soxhlet extraction with methanol.

The porosity in these materials was tested by collecting the nitrogen gas adsorption and desorption isotherms at 77 K from which the BET surface area was calculated. A comparison of these BET surface areas is shown in Figure 1. Further porosity data is provided in Table 1. From these data, it is clear that porosity is greatly affected by the choice of polymerization solvent for many of these networks. Network **1**—our first CMP material, CMP-1²¹—was found to be relatively insensitive to the solvent choice, with BET surface areas of 867, 837, and 941 m²/g in toluene, DMF, and THF, respectively. A slight decrease to 609 m²/g occurred when the polymerization was carried out in 1,4-dioxane. By contrast, other networks exhibited quite different BET surface areas depending on the polymerization solvent. For example, **9**, a nitrated variant of CMP-1, was found to have a BET surface area of 967 and 823 m²/g in DMF and 1,4-dioxane, respectively, but only 247 and 335 m²/g in toluene and THF. The highest surface area was found for network **8**, a partially fluorinated material, which exhibited a BET surface area of 1260 m²/g when synthesized in DMF. A mean BET surface area calculated over the 11 different networks shows the following trend in terms of surface area obtained: DMF > THF > 1,4-dioxane > toluene. As such, toluene (our original solvent choice for these systems)^{21,28} is certainly not optimal. Indeed, Figure 1b shows that DMF gives rise to higher surface areas in 10 of the 11 networks in comparison with toluene. In three cases, more than a 3-fold enhancement in surface area is observed when DMF is used.

The pore volume in the materials was also calculated from the nitrogen isotherms. The pore volume at $P/P_0 = 0.1$ gives a good approximation of the micropore volume ($V_{0.1}$), as described previously²⁸ (Table 1). The mean micropore volume for the networks followed this trend: DMF > 1,4-dioxane > THF > toluene. That is, DMF was again the best overall choice and toluene the worst. The micropore volume divided by the total pore volume ($V_{0.1/\text{tot}}$) gives an indication of how microporous the material is—that is, how much of the pore volume arises from micropores rather than mesopores or interparticulate porosity. Again, the trend in terms of reaction solvents was DMF > 1,4-dioxane > THF > toluene. It is therefore clear that the use of

Table 1. BET Surface Areas, Pore Volumes, and Microanalysis of Networks Synthesized in Different Solvents

	Dibromo monomer	Solvent	SA_{BET}	$V_{0.1}$	V_{tot}	$V_{0.1/\text{tot}}$
			(m^2/g) ^a	(cm^3/g) ^b	(cm^3/g) ^c	
1		Toluene	867	0.33	0.99	0.33
		DMF	837	0.32	0.45	0.71
		THF	941	0.36	1.24	0.29
		Dioxane	609	0.23	0.36	0.64
2		Toluene	204	0.09	0.43	0.21
		DMF	744	0.29	0.55	0.53
		THF	734	0.28	0.68	0.41
		Dioxane	744	0.29	0.55	0.53
3		Toluene	136			
		DMF	550	0.21	0.37	0.57
		THF	716	0.28	1.05	0.27
		Dioxane	573	0.22	0.60	0.37
4		Toluene	344	0.09	0.17	0.53
		DMF	742	0.28	0.70	0.40
		THF	522	0.20	0.52	0.38
		Dioxane	580	0.22	0.67	0.33
5		Toluene	436	0.08	0.13	0.62
		DMF	599	0.23	0.44	0.52
		THF	532	0.21	0.49	0.43
		Dioxane	638	0.25	0.83	0.30
6		Toluene	761	0.27	1.73	0.16
		DMF	1043	0.40	0.71	0.56
		THF	847	0.33	0.69	0.48
		Dioxane	778	0.32	0.65	0.49
7		Toluene	682	0.25	1.06	0.24
		DMF	899	0.34	0.75	0.45
		THF	985	0.38	1.09	0.35
		Dioxane	1022	0.40	0.88	0.45
8		Toluene	690	0.27	0.52	0.52
		DMF	1260	0.48	0.88	0.55
		THF	639	0.25	0.41	0.61
		Dioxane	869	0.39	0.61	0.64
9		Toluene	247	0.07	0.18	0.39
		DMF	967	0.37	0.94	0.39
		THF	335	0.13	0.17	0.76
		Dioxane	823	0.40	0.60	0.67
10		Toluene	542	0.20	0.97	0.21
		DMF	653	0.25	0.36	0.69
		THF	994	0.38	0.97	0.39
		Dioxane	611	0.23	0.47	0.49
11		Toluene	779	0.29	1.40	0.21
		DMF	1056	0.40	0.77	0.52
		THF	1014	0.39	0.99	0.39
		Dioxane	727	0.28	0.74	0.38

^a BET surface area calculated over the pressure range 0.01–0.05 P/P_0 . ^b $V_{0.1}$ = pore volume at $P/P_0 = 0.1$. ^c V_{tot} total pore volume calculated at $P/P_0 = 0.99$.

DMF as reaction solvent leads to materials with substantially higher average surface areas and that this effect arises primarily from enhanced micropore volume, rather than for example a change in the particulate morphology. The use of THF and dioxane leads to materials with similar properties: on average, THF gives rise to slightly higher average BET surface areas, and dioxane leads to a slightly higher proportion of micropores.

The difference in the nature of the porosity in the networks is exemplified by networks **1**, **3**, **7**, and **9**, as shown in Figure 2. The nitrogen isotherms for **1** show that materials synthesized in DMF or THF exhibited a type I isotherm. When synthesized in toluene or 1,4-dioxane, **1** gives rise to a type IV isotherm, indicative of mesopores and/or small macropores, although we would point out that a type I isotherm was observed when **1** was synthesized in toluene from the more reactive 1,4-diiodobenzene monomer.^{21,25}

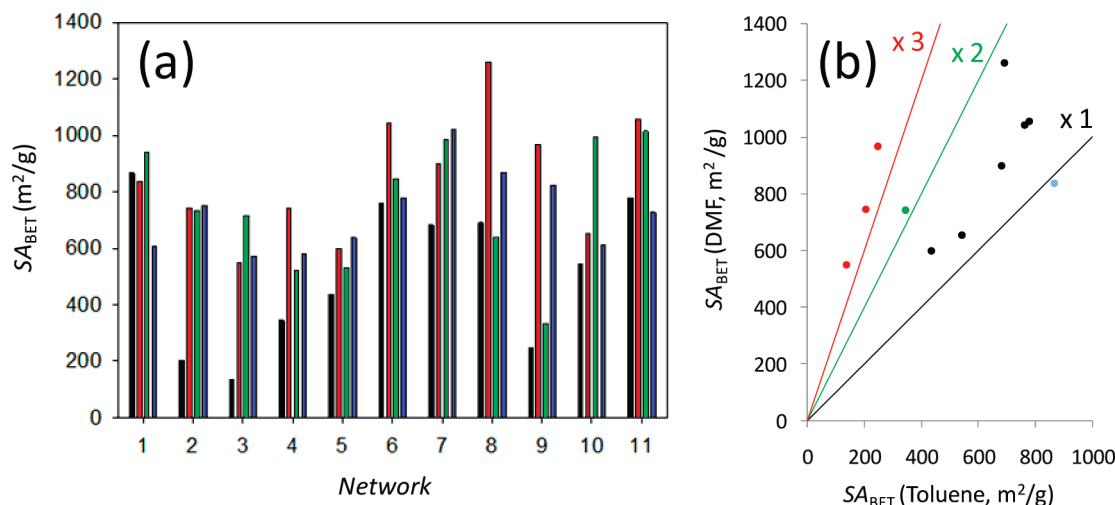


Figure 1. (a) BET surface area (SA_{BET}) for CMP networks synthesized in toluene (black), DMF (red), THF (green), and dioxane (blue). (b) Plot showing comparison of SA_{BET} for networks synthesized in toluene and DMF; lines are shown for guidance representing equivalent surface area (black), double surface area (green), and triple surface area in toluene (red)—that is, 3 of the 11 networks (red symbols) have more than a 3-fold increase in surface area when synthesized in DMF instead of toluene. All networks show an increase in SA_{BET} when prepared in DMF apart from 1 (blue symbol) which is, within error, unchanged.

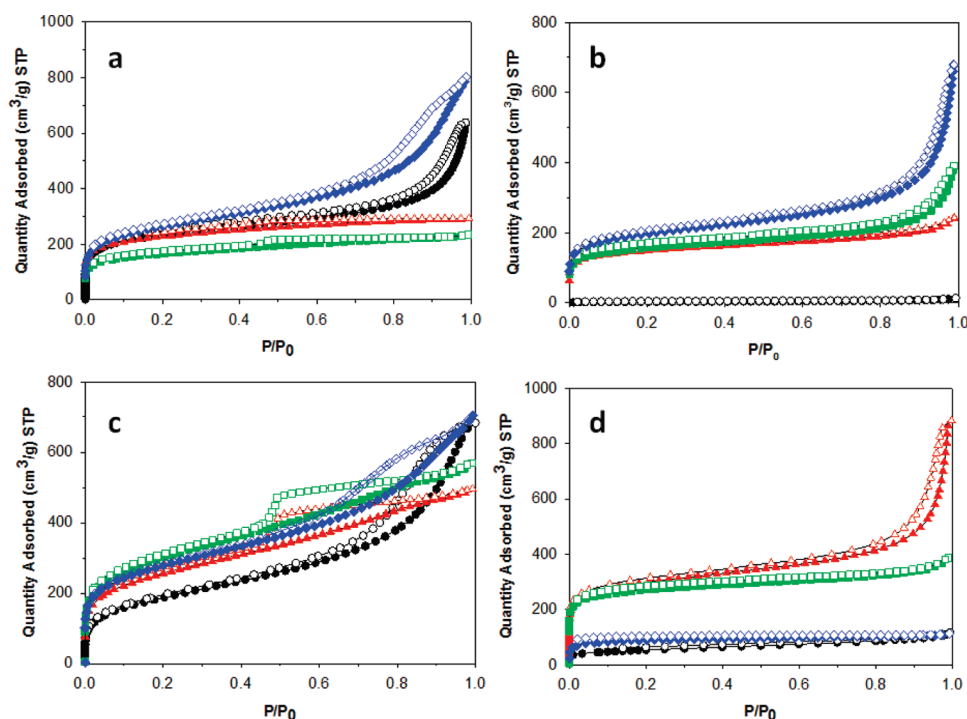


Figure 2. Nitrogen adsorption (closed symbols) and desorption (open symbols) isotherms for networks 1 (a), 3 (b), 7 (c), and 9 (d) synthesized in toluene (black circles), DMF (red triangles), dioxane (green squares), and THF (blue diamonds) collected at 77.3 K.

Similarly, network 3 shows a type I isotherm when synthesized in DMF, with some type IV character when synthesized in 1,4-dioxane and more type IV character when synthesized in THF. In toluene, an almost nonporous material was formed. Network 7 shows type IV isotherms in all solvents although the nature of the hysteresis loop varies depending on the solvent medium. Network 9 shows a significantly larger micropore step when synthesized in DMF or 1,4-dioxane as compared to THF and toluene. The network synthesized in DMF shows some type IV character, unlike the analogous material prepared in DMF. Isotherms for the other networks are shown in the Supporting Information. For network 9, we examined the effect of monomer stoichiometry and reaction temperature on the final networks synthesized in DMF. In agreement with our previous results,²⁵ the highest surface area

materials resulted from a monomer stoichiometry utilizing a 0.5 M excess of ethynyl groups (see Supporting Information). Additionally, lower surface area materials were prepared at this monomer ratio at lower reaction temperatures (see Supporting Information).

To attempt to explain these results, we examined a subset of the networks (1, 3, 7, and 9) by solid-state NMR to identify any differences at the molecular level between networks prepared in DMF and toluene. Figure 3 shows the ^1H – ^{13}C CP/MAS NMR spectra of these networks. Functional group incorporation was confirmed for networks 7 and 9 by their characteristic peaks at ca. 20 ppm ($\text{C}_{\text{Ar}}\text{CH}_3$) and 149 ppm ($\text{C}_{\text{Ar}}\text{--NO}_2$), respectively. The assignment of the peaks is consistent with the CP kinetics shown in the Supporting Information.

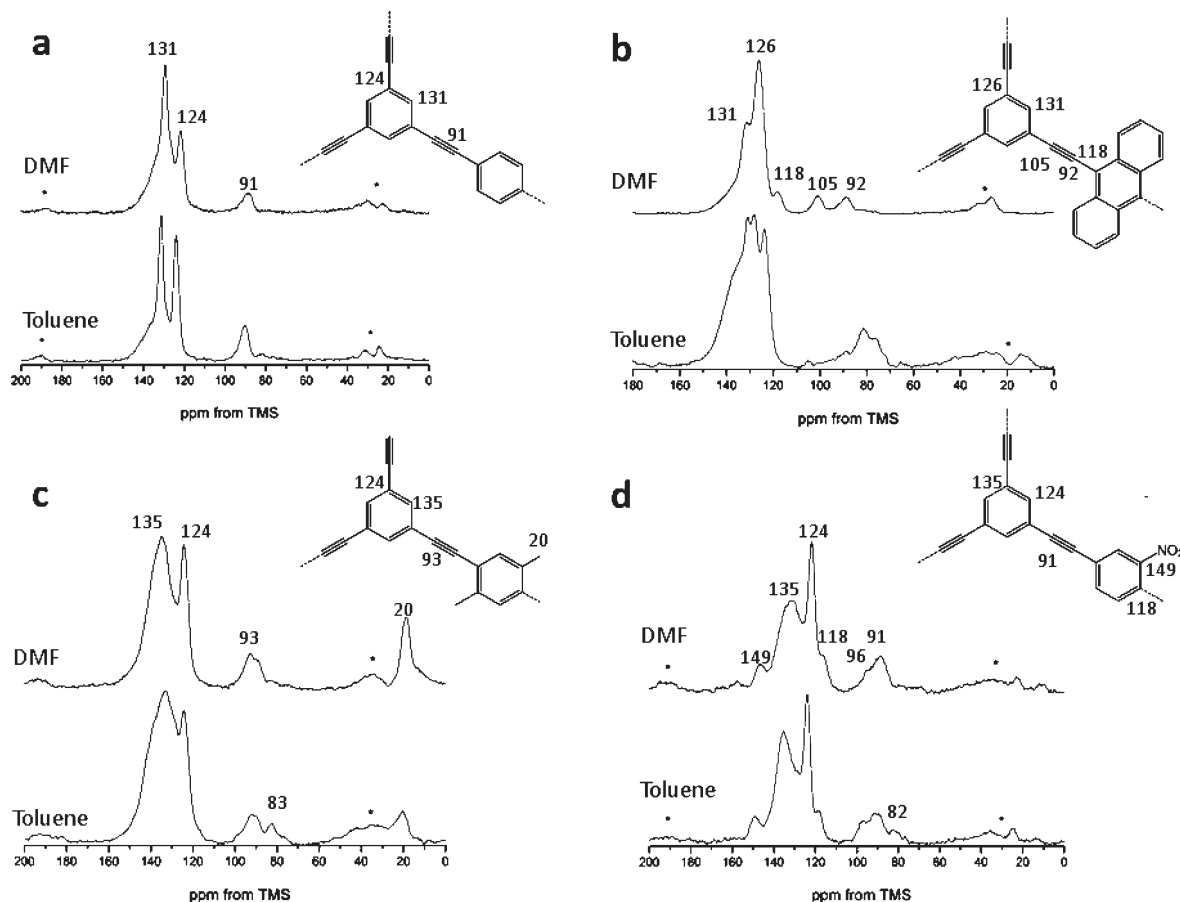


Figure 3. ^1H – ^{13}C CP/MAS NMR spectra of networks **1** (a), **3** (b), **7** (c), and **9** (d) recorded at a spinning speed of 10 kHz. Asterisks denote spinning sidebands. Insets show structures and peak assignments.

Table 2. Ratio of Integration of Terminal:Quaternary Alkyne As Determined from Solid State NMR Data Shown in Figure 3

network	alkyne ratio in toluene	alkyne ratio in DMF
1	0.40	0.16
3	3.31	0.07
7	0.19	≈ 0
9	0.15	≈ 0

All of the networks show aromatic peaks at ca. 131 ($\text{C}_{\text{Ar}}\text{--H}$) and 124 ppm ($\text{C}_{\text{Ar}}\text{--C}\equiv\text{C}\text{--}$) and peaks at ca. 90 ppm ($\text{C}_{\text{Ar}}\text{--C}\equiv\text{C}\text{--}$) for quaternary alkynes and 82 ppm ($\text{C}_{\text{Ar}}\text{--C}\equiv\text{C}\text{--H}$) for terminal alkynes, consistent with our previous work.^{19,22,23} In order to probe the level of polycondensation for the networks, each spectrum was deconvoluted (see Supporting Information, Figures S2.1–2.8) and the ratio of terminal/quaternary alkyne was calculated (see Table 2).²³ All networks were found to have a lower terminal/quaternary alkyne ratio in DMF than in toluene, indicating that there is a higher degree of condensation in the networks synthesized in DMF compared to those prepared in toluene. This is corroborated by CHN analysis, where networks synthesized in DMF consistently exhibit values that are significantly closer to those calculated for hypothetical fully condensed networks (see Supporting Information). The changes in the ratio of aromatic peaks for the network **1** are also consistent with a higher degree of condensation in DMF than in toluene. Compared with the network prepared in toluene, network **1** synthesized in DMF shows a higher population for the ($\text{C}_{\text{Ar}}\text{--H}$) peak at 131 ppm. This is due to an increased proportion of $\text{--C}_6\text{H}_4\text{--}$ linkages in the network.

Network **9** was shown to have unreacted bromine end groups. The $\text{C}_{\text{Ar}}\text{--Br}$ signal appears at 96 ppm, and the relative population of bromine end groups is higher in DMF (0.64) than in

toluene (0.50). This could perhaps indicate that the network preferentially terminates with alkyne end groups in toluene, whereas in DMF the network preferentially terminates with the bromine end group.

Scanning electron microscopy for these networks also provides useful morphological information to explain the observed porosity (Figure 4). For **1**, a similar morphology is observed when prepared in either toluene or DMF (Figure 1a). For **3**, the material synthesized in toluene shows the presence of large, fused polymeric masses, as described previously.²⁸ These are absent in the network synthesized in DMF, and the material has similar morphology to many other high surface area CMP networks (Figure 1b).^{21,25,31} Network **7** also shows a similar morphology when synthesized in both toluene and DMF (Figure 1c). Like **3**, network **9** also shows a strong difference in porosity when synthesized in toluene or DMF, and it too comprises larger fused masses when synthesized in toluene (Figure 1d). In DMF, the morphology is similar to that observed for networks **1** and **7**. Similar morphology trends were observed by SEM for the other networks, with those exhibiting lower surface areas also tending to showing the presence of larger fused masses of polymeric material (see Figures S3.1–3.35, Supporting Information).

Combining the NMR and SEM data, it appears that the degree of condensation in these networks is affected by the choice of reaction solvent. Increased condensation in the network leads to phase separation into materials with different pore structures and different morphologies. Presumably, networks with higher degrees of condensation are less able to collapse and densify, thus leading to higher levels of microporosity. Choice of solvent was shown by others⁴⁸ to be key for other cross-coupling reactions, with the polarity of the solvent playing a particularly important

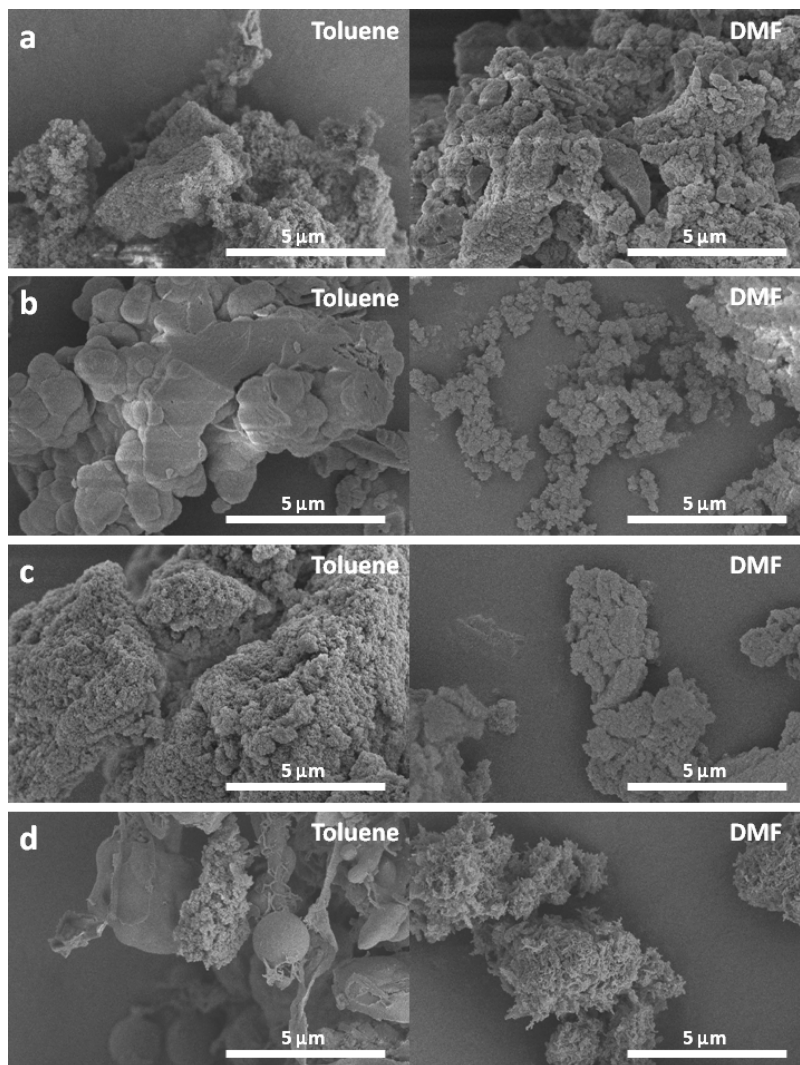


Figure 4. SEM of networks synthesized in toluene (left-hand column) and DMF (right-hand column): (a) network 1, (b) network 3, (c) network 7, and (d) network 9.

role. For example, higher conversions were observed in more polar solvents for reactions of bromotoluene with a number of alkynes. In general, we find that higher surface area networks are prepared in DMF. For some systems such as large fused aromatics, the increase in polycondensation in DMF might also be due to improved solubility of the monomers in this solvent. Indeed, the solid state NMR spectrum of **3** shows the largest difference in alkyne ratio between the networks synthesized in DMF and toluene. Indeed, it is possible to suggest that network **3** synthesized in toluene is to some extent a homocoupled network²⁴ with entrained anthracene monomer, particularly since the peak at ca. 135 ppm is especially broad. There is also an absence of a peak at 118 ppm which is indicative of coupling and present in the spectrum of **3** synthesized in DMF.

Conclusions

We have shown that the surface area and microporosity in polymer networks prepared via $A_3 + B_2$ Sonogashira–Hagihara coupling are strongly affected by the choice of the reaction solvent. Toluene is a relatively poor solvent, resulting in materials with low surface areas and type IV isotherms. By contrast, solvents such as DMF, 1,4-dioxane, and THF are all suitable for these polymerizations. In general, networks formed in DMF tend to exhibit the highest surface areas and the highest levels of microporosity, although THF is superior for certain networks. These results are

important because they illustrate that solvent choice may be a prime factor in the synthesis of new CMPs for specific applications. We would suggest that researchers in this area invest some time in the evaluation of different reaction solvents when new CMP materials are prepared. As these results suggest, it is likely that there is no “universal” solvent which is optimal for porosity in these networks. Large gains in surface area are possible in some cases.

Acknowledgment. We thank the Engineering and Physical Sciences Research Council (EPSRC; EP/F057865/1 and EP/C511794/1) for funding. A.I.C. is a Royal Society Wolfson Merit Award holder. We thank NWDA and the European Union Objective 1 Programme for supporting the establishment of the Centre for Materials Discovery.

Supporting Information Available: Nitrogen adsorption/desorption isotherms, solid state NMR, SEM images, infrared spectra, elemental analysis, and effect of bromo:alkyne ratio and reaction temperature. This material is available free of charge via the Internet at <http://pubs.acs.org>.

References and Notes

- (1) Budd, P. M.; Butler, A.; Selbie, J.; Mahmood, K.; McKeown, N. B.; Ghanem, B.; Msayib, K.; Book, D.; Walton, A. *Phys. Chem. Chem. Phys.* **2007**, *9*, 1802.

- (2) Furukawa, H.; Yaghi, O. M. *J. Am. Chem. Soc.* **2009**, *131*, 8875.
- (3) Wood, C. D.; Tan, B.; Trewin, A.; Niu, H. J.; Bradshaw, D.; Rosseinsky, M. J.; Khimyak, Y. Z.; Campbell, N. L.; Kirk, R.; Stockel, E.; Cooper, A. I. *Chem. Mater.* **2007**, *19*, 2034.
- (4) Svec, F.; Germain, J.; Fréchet, J. M. J. *Small* **2009**, *5*, 1098.
- (5) McKeown, N. B.; Budd, P. M. *Chem. Soc. Rev.* **2006**, *35*, 675.
- (6) Ghanem, B. S.; McKeown, N. B.; Budd, P. M.; Al-Harbi, N. M.; Fritsch, D.; Heinrich, K.; Starannikova, L.; Tokarev, A.; Yampolskii, Y. *Macromolecules* **2009**, *42*, 7881.
- (7) Schmidt, J.; Weber, J.; Epping, J. D.; Antonietti, M.; Thomas, A. *Adv. Mater.* **2009**, *21*, 702.
- (8) McKeown, N. B.; Budd, P. M.; Msayib, K. J.; Ghanem, B. S.; Kingston, H. J.; Tattershall, C. E.; Makhseed, S.; Reynolds, K. J.; Fritsch, D. *Chem.—Eur. J.* **2005**, *11*, 2610.
- (9) Budd, P. M.; McKeown, N. B.; Fritsch, D. *J. Mater. Chem.* **2005**, *15*, 1977.
- (10) Budd, P. M.; Ghanem, B. S.; Makhseed, S.; McKeown, N. B.; Msayib, K. J.; Tattershall, C. E. *Chem. Commun.* **2004**, 230.
- (11) McKeown, N. B.; Budd, P. M. *Macromolecules* **2010**, *43*, 5163.
- (12) Tsyurupa, M. P.; Davankov, V. A. *React. Funct. Polym.* **2006**, *66*, 768.
- (13) Lee, J. Y.; Wood, C. D.; Bradshaw, D.; Rosseinsky, M. J.; Cooper, A. I. *Chem. Commun.* **2006**, 2670.
- (14) Germain, J.; Hradil, J.; Fréchet, J. M. J.; Svec, F. *Chem. Mater.* **2006**, *18*, 4430.
- (15) Ahn, J. H.; Jang, J. E.; Oh, C. G.; Ihm, S. K.; Cortez, J.; Sherrington, D. C. *Macromolecules* **2006**, *39*, 627.
- (16) Wood, C. D.; Tan, B.; Trewin, A.; Su, F.; Rosseinsky, M. J.; Bradshaw, D.; Sun, Y.; Zhou, L.; Cooper, A. I. *Adv. Mater.* **2008**, *20*, 1916.
- (17) Côté, A. P.; El-Kaderi, H. M.; Furukawa, H.; Hunt, J. R.; Yaghi, O. M. *J. Am. Chem. Soc.* **2007**, *129*, 12914.
- (18) El-Kaderi, H. M.; Hunt, J. R.; Mendoza-Cortes, J. L.; Côté, A. P.; Taylor, R. E.; O’Keeffe, M.; Yaghi, O. M. *Science* **2007**, *316*, 268.
- (19) Côté, A. P.; Benin, A. I.; Ockwig, N. W.; O’Keeffe, M.; Matzger, A. J.; Yaghi, O. M. *Science* **2005**, *310*, 1166.
- (20) Uribe-Romo, F. J.; Hunt, J. R.; Furukawa, H.; Klock, C.; O’Keeffe, M.; Yaghi, O. M. *J. Am. Chem. Soc.* **2009**, *131*, 4570.
- (21) Jiang, J.-X.; Su, F.; Trewin, A.; Wood, C. D.; Campbell, N. L.; Niu, H.; Dickinson, C.; Ganin, A. Y.; Rosseinsky, M. J.; Khimyak, Y. Z.; Cooper, A. I. *Angew. Chem., Int. Ed.* **2007**, *46*, 8574.
- (22) Cooper, A. I. *Adv. Mater.* **2009**, *21*, 1291.
- (23) Weber, J.; Thomas, A. *J. Am. Chem. Soc.* **2008**, *130*, 6334.
- (24) Jiang, J.-X.; Su, F.; Niu, H.; Wood, C. D.; Campbell, N. L.; Khimyak, Y. Z.; Cooper, A. I. *Chem. Commun.* **2008**, 486.
- (25) Jiang, J.-X.; Su, F.; Trewin, A.; Wood, C. D.; Niu, H.; Jones, J. T. A.; Khimyak, Y. Z.; Cooper, A. I. *J. Am. Chem. Soc.* **2008**, *130*, 7710.
- (26) Dawson, R.; Su, F. B.; Niu, H. J.; Wood, C. D.; Jones, J. T. A.; Khimyak, Y. Z.; Cooper, A. I. *Macromolecules* **2008**, *41*, 1591.
- (27) (a) Jiang, J.-X.; Trewin, A.; Su, F.; Wood, C. D.; Niu, H.; Jones, J. T. A.; Khimyak, Y. Z.; Cooper, A. I. *Macromolecules* **2009**, *42*, 2658. (b) Jiang, J.-X.; Laybourn, A.; Clowes, R.; Khimyak, Y. Z.; Bacsá, J.; Higgins, S. J.; Adams, D. J.; Cooper, A. I. *Macromolecules*, **2010**, DOI: 10.1021/ma101468r.
- (28) Dawson, R.; Laybourn, A.; Clowes, R.; Khimyak, Y. Z.; Adams, D. J.; Cooper, A. I. *Macromolecules* **2009**, *42*, 8809.
- (29) Schmidt, J.; Weber, J.; Epping, J. D.; Antonietti, M.; Thomas, A. *Adv. Mater.* **2009**, *21*, 702.
- (30) Schmidt, J.; Werner, M.; Thomas, A. *Macromolecules* **2009**, *42*, 4426.
- (31) Stöckel, E.; Wu, X. F.; Trewin, A.; Wood, C. D.; Clowes, R.; Campbell, N. L.; Jones, J. T. A.; Khimyak, Y. Z.; Adams, D. J.; Cooper, A. I. *Chem. Commun.* **2009**, 212.
- (32) Choi, J. H.; Choi, K. M.; Jeon, H. J.; Choi, Y. J.; Lee, Y.; Kang, J. K. *Macromolecules* **2010**.
- (33) Yuan, S. W.; Dorney, B.; White, D.; Kirklin, S.; Zapol, P.; Yu, L. P.; Liu, D. J. *Chem. Commun.* **2010**, 4547.
- (34) Chen, L.; Yang, Y.; Jiang, D. L. *J. Am. Chem. Soc.* **2010**, *132*, 9138.
- (35) Ben, T.; Ren, H.; Ma, S. Q.; Cao, D. P.; Lan, J. H.; Jing, X. F.; Wang, W. C.; Xu, J.; Deng, F.; Simmons, J. M.; Qiu, S. L.; Zhu, G. S. *Angew. Chem., Int. Ed.* **2009**, *48*, 9457.
- (36) Du, X.; Sun, Y. L.; Tan, B. E.; Teng, Q. F.; Yao, X. J.; Su, C. Y.; Wang, W. *Chem. Commun.* **2010**, 46, 970.
- (37) Ren, H.; Ben, T.; Wang, E. S.; Jing, X. F.; Xue, M.; Liu, B. B.; Cui, Y.; Qiu, S. L.; Zhu, G. S. *Chem. Commun.* **2010**, 46, 291.
- (38) Chen, L.; Honsho, Y.; Seki, S.; Jiang, D. L. *Angew. Chem., Int. Ed.* **2010**, *132*, 6742.
- (39) Hasell, T.; Wood, C. D.; Clowes, R.; Jones, J. T. A.; Khimyak, Y. Z.; Adams, D. J.; Cooper, A. I. *Chem. Mater.* **2010**, *22*, 557.
- (40) Li, A.; Lu, R. F.; Wang, Y.; Wang, X.; Han, K. L.; Deng, W. Q. *Angew. Chem., Int. Ed.* **2010**, *49*, 3330.
- (41) Sing, K. S. W.; Everett, D. H.; Haul, R. A. W.; Moscou, L.; Pierotti, R. A.; Rouquerol, J.; Siemieniowska, T. *Pure Appl. Chem.* **1985**, *57*, 603.
- (42) Chinchilla, R.; Najera, C. *Chem. Rev.* **2007**, *107*, 874.
- (43) Bunz, U. H. F. *Chem. Rev.* **2000**, *100*, 1605.
- (44) Sherrington, D. C. *Chem. Commun.* **1998**, 2275.
- (45) Bennett, A. E.; Rienstra, C. M.; Auger, M.; Lakshmi, K. V.; Griffin, R. G. *J. Chem. Phys.* **1995**, *103*, 6951.
- (46) Kolodziejski, W.; Klinowski, J. *Chem. Rev.* **2002**, *102*, 613.
- (47) (a) Campbell, N. L.; Clowes, R.; Ritchie, L. K.; Cooper, A. I. *Chem. Mater.* **2009**, *21*, 204. (b) Ritchie, L. K.; Trewin, A.; Reguera-Galan, A.; Hasell, T.; Cooper, A. I. *Microporous Mesoporous Mater.* **2010**, *132*, 132.
- (48) Novák, Z.; Szabó, A.; Répási, J.; Kotschy, A. *J. Org. Chem.* **2003**, *68*, 3327.